Substituent and Matrix Effects on the Excited Triplet States of 1,4-Naphthoquinones

Takuji Shimokage, Tadaaki Ikoma, Kimio Akiyama, and Shozo Tero-Kubota*

Institute for Chemical Reaction Science, Tohoku University, Katahira 2-1, Aobaku, Sendai 980-77, Japan

Minoru Yamaji and Haruo Shizuka

Department of Chemistry, Gunma University, Kiryu, Gunma 376, Japan

Received: June 4, 1997; In Final Form: August 14, 1997[⊗]

Phosphorescence and TREPR spectra have been measured for 2-methyl-1,4-naphthoquinone (MNQ), 2,3-dimethyl-1,4-naphthoquinone (DMNQ), and 2-methoxynaphthoquinone (MeONQ) in several matrices at low temperatures. The $|D|$ value of ZFS parameter decreases with increasing the electron-donating character of the substituent group. For MNQ, the T_1 state is clearly assigned to be $^3n\pi^*$ in character. The broad phosphorescence spectra and minor effects of the matrix polarity on the ZFS parameters lead to the conclusion that the character of the T_1 states are mainly $^3\pi\pi^*$ in DMNQ and MeONQ. The T_1 states of the present naphthoquinone derivatives have more or less mixed character of the $^3n\pi^*$ and $^3\pi\pi^*$ states.

1. Introduction

Photophysics and photochemistry of 1,4-naphthoquinones have been a subject of study for a long time.[1] Studies by emission and absorption spectroscopies made a fundamental contribution to our understanding of the electronic structure of their excited states.[2−4] The primary photochemical processes have been also investigated very actively by CIDEP[5,6] and laser flash photolysis spectroscopies.[7−10] However, little is known of the ZFS parameters of the T_1 states of 1,4-naphthoquinone (NQ) and its derivatives. Using a time-resolved EPR (TREPR) technique, a very large zero-field splitting (ZFS) constant of $|D| = 0.33$ cm^{-1} was determined for the T_1 state of NQ in polar solvents.[11] The large $|D|$ value is probably due to coupling of the $T_1(^3n\pi^*)$ and upper lying $^3\pi\pi^*$ states through spin−orbit interaction. In a neat crystal of NQ, the T_1 state is ascribed to a superposition of the two $n\pi^*$ states of the free molecule, indicating a large intermolecular interaction between the nearest neighbor molecules.[12] It can be expected that the electronic structure of the triplet state naphthoquinones depends on the substituents and also is influenced by matrices, because they have relatively small energy differences between the $^3n\pi^*$ and $^3\pi\pi^*$ states. In the previous work, we reported that the T_1 states of *o*-quinones such as 1,2-naphthoquinone and 9,10-phenanthrenequinone were significantly affected by matrix polarity.[13]

It is well-known that solvent polarity affects the electronic structure of the excited triplet states of carbonyl compounds. The T_1 state characters of the carbonyl molecules with small energy separation between the $^3n\pi^*$−$^3\pi\pi^*$ states are significantly sensitive to the matrix polarity.[14−22] On the other hand, for benzophenone, the complex formation with water is essential to change the T_1 state character from $^3n\pi^*$ to mixed $^3n\pi^*$−$^3\pi\pi^*$.[23,24] The energy levels of $^3n\pi^*$ states are destabilized more than those of $^3\pi\pi^*$ by the solvation with polar molecules or hydrogen bond formation with protic solvents.

In the present paper, we have investigated the T_1 states of 2-methyl-1,4-naphthoquinone (MNQ), 2,3-dimethyl-1,4-naphthoquinone (DMNQ), and 2-methoxynaphthoquinone (MeONQ) by emission and time-resolved EPR (TREPR) spectroscopies (Figure 1). Matrix effects on the phosphorescence and TREPR spectra have been measured.

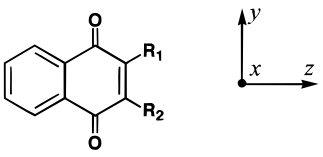

	R_1	R_2
NQ	H	H
MNQ	CH_3	H
DMNQ	CH_3	CH_3
MeONQ	OCH_3	H

Figure 1. Molecular structure and principal axes of 1,4-naphthoquinones.

The triplet EPR spectra are interpreted by the following spin Hamiltonian:

$$H = g\beta\mathbf{B}\cdot\mathbf{S} + \mathbf{S}\cdot\mathbf{D}\cdot\mathbf{S}$$
$$= g\beta\mathbf{B}\cdot\mathbf{S} - XS_x^2 - YS_y^2 - ZS_z^2$$
$$= g\beta\mathbf{B}\cdot\mathbf{S} + D[S_z^2 - (1/3)S^2] + E[S_x^2 - S_y^2]$$

where **D** is the ZFS tensor with principal values ($-X$, $-Y$, and $-Z$). D and E describe the ZFS parameters that are related to ($-X$, $-Y$, and $-Z$) by $D = -3Z/2$ and $E = (Y - X)/2$. The anisotropy of the g tensor could be neglected in the analysis of the TREPR spectra in the present system.

2. Experimental Section

NQ and MNQ were purchased from Wako Chem. and Tokyo Kasei Co., respectively. DMNQ was kindly donated from Eisai Chemical Co., Ltd. MeONQ was prepared according to the procedures reported previously.[25] NQ and DMNQ were purified by passing through a silica gel column with benzene. MNQ and MeONQ were carefully purified by recrystallization from ethanol in the dark. Since the presence of water in solvents gave drastic effects on the phosphorescence and TREPR spectra, solvents were all carefully dehydrated. Spectrograde solvents (Nacalai) of toluene and *n*-hexane were degassed by freeze-pump-thaw cycles and dehydration using sodium metal. Methylcyclohexane (MCH, Aldrich, Spectrograde) was degassed and

[⊗] Abstract published in *Advance ACS Abstracts,* November 15, 1997.

S1089-5639(97)01818-5 CCC: $14.00

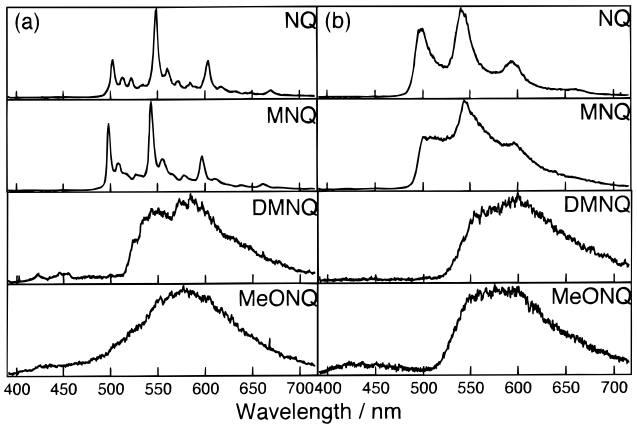

Figure 2. Phosphorescence spectra of NQ and its derivatives in *n*-hexane (a) and absolute ethanol (b) matrices at 77 K. The spectrum of MeONQ was observed at 8 μs after the laser photolysis and the others were measured at 500 μs. See text for detail.

stored on molecular sieves 4A (Nacalai). Spectrograde solvent of 2-methyltetrahydrofuran (MTHF, Aldrich) was purified by passing through a basic alumina column and distillation, followed by dehydration with sodium metal. Absolute ethanol (Wako), which was obtained by reflux with Mg metal for 48 h, was degassed by freeze−pump−thaw cycles and stored over molecular sieve 4A in a vacuum line.

The phosphorescence spectra were recorded using the multichannel analyzer controlled by a personal computer. A diode array (Princeton Instruments, IRY-700) was triggered and gated by the combined system of a digital delay/pulse generator (Stanford Research, DG-535), a pulse generator (Princeton Instruments, FG-100), and a personal computer (NEC PC-9801 BA). The transient signals were accumulated eight times on the computer. A Nd:YAG laser (Quanta-Ray GCR-14, 355 nm) was used as the light source. Measurements of the emission spectra were performed with the concentration of 10^{-4} mol dm^{-3} of the quinones. TREPR measurements were carried out by using a Varian X-band EPR spectrometer without magnetic field modulation as reported previously.[26] A helium cryostat (Oxford ESR-900) was utilized for the measurements at very low temperatures. An excimer laser (XeCl 308 nm, Lumonics HE-420) was used as the light pulse source. TREPR measurements were performed with the concentration of 10^{-2}−10^{-3} mol dm^{-3} of quinones.

3. Results

Phosphorescence Spectra. Figure 2a depicts the phosphorescence spectra of NQ and its derivatives in a *n*-hexane matrix at 77 K. NQ (λ_{00} = 503 nm) and MNQ (λ_{00} = 498 nm) showed characteristic ^{3}nπ^* phosphorescence spectra. These spectra agree well with those reported previously.[2] For DMNQ (λ_{00} = 521 nm) and MeONQ (λ_{max} = 578 nm), relatively red-shifted and broad phosphorescence spectra were observed in hexane at 77 K. The 00 energy for DMNQ was estimated from the phosphorescence shoulder. The very weak emission observed in the wavelength region shorter than 500 nm is considered to be due to the photoreaction products, because the intensity increases with increasing the laser photolysis.

In order to examine hydrogen-bonding effects, the phosphorescence spectra in an absolute ethanol matrix were measured (Figure 2b). The spectra of NQ and MNQ show well-resolved vibrational structures though they are slightly broadened compared with those in a hexane matrix. The red-shifted spectrum of DMNQ may be induced by hydrogen-bonding ethanol molecules. The very weak emission bands observed in the wavelength region shorter than 500 nm in the spectra of the naphthoquinone derivatives are due to the unknown photoreaction products.

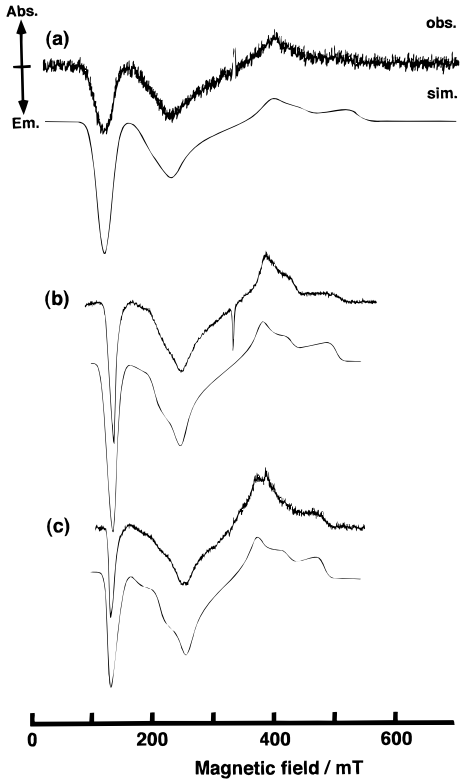

Figure 3. TREPR spectra of MNQ, DMNQ, and MeONQ observed at 0.5 μs after the laser pulse in an MTHF matrix at 77 K.

The phosphorescence lifetime was measured for MeONQ in a methanol/ethanol (1:1, v/v) matrix at 77 K where those of NQ, MNQ, and DMNQ were previously reported to be 0.14, 0.84, and 1.4 ms, respectively.[7,9] The lifetime of 4.2 ms was obtained for MeONQ. These values indicate that the phosphorescence lifetimes increases with increase of the electron-donating character of the substituent group on naphthoquinones.

TREPR Spectra. As shown in Figure 3, the TREPR spectra of MNQ, DMNQ, and MeONQ were clearly observed in an MTHF matrix at 77 K. The strong emissive signals around 0.13 T correspond to the $|\Delta M_S| = 2$ transition. The $|\Delta M_S| = 1$ transitions show the spin polarization of EEE at the low-field half and AAA at the high-field half, where E and A represent emission and absorption of microwave, respectively. We could not obtain the TREPR spectrum of NQ in an MTHF matrix even at 4 K. This is probably ascribable to the large value of the ZFS parameters due to strong spin−orbit interaction.

It is reasonable to assume that the spin-orbit interaction due to the carbonyl oxygen atoms plays an important role for the intersystem crossing (ISC) process from the S_1 state to the T_1 state of the present quinones. Therefore, the T_y sublevel would be mainly populated in the ISC process, where the *y* axis is parallel to the carbonyl bonds (see Figure 1). From the observed polarization pattern (EEEE/AAA), we tentatively conclude that the preferentially populated T_y sublevel is the highest one. Although the in-plane principal (*y* and *z*) axes are ambiguous for MNQ and MeONQ because of their low symmetry, the deviation is considered to be small. The speculation would be reasonable because the present quinones show the same relative population difference in the triplet sublevels through the ISC as described below. The TREPR spectra observed were well reproduced by computer simulation (Figure 3). The $|D|$ values determined were 0.195, 0.169, and 0.145 cm^{-1} for MNQ, DMNQ, and MeONQ, respectively. The line shape of the Gaussian type was used to reproduce the observed TREPR

TABLE 1: ZFS Parameters (D^a and E^b in cm^{-1}) of 1,4-Naphthoquinone Derivatives in Several Matrices at Very Low Temperatures

	MCH		toluene		MTHF		absolute ethanol	
	D	*E*	*D*	*E*	*D*	*E*	*D*	*E*
MNQ	−0.199	0.0165	−0.176	0.0102	−0.195	0.0165	−0.215	0.0170
DMNQ	−0.169	0.0145	−0.161	0.0143	−0.169	0.0145	−0.173	0.0162
MeONQ	−0.135	0.0165	−0.140	0.0165	−0.145	0.0155	−0.155	0.0165

[a] $D = -(3/2)\ Y$. [b] $E = -(1/2)(X - Z)$.

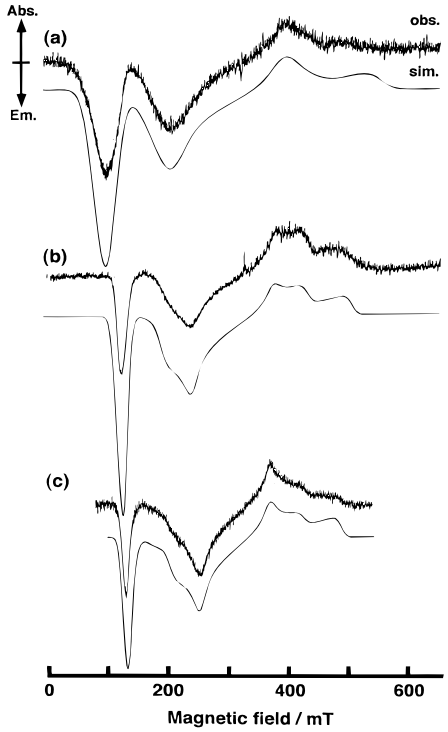

Figure 4. TREPR spectra of MNQ, DMNQ, and MeONQ observed at 0.5 μs after the laser pulse in an absolute ethanol matrix at 30 K.

spectra. The line width is larger in MNQ (14 mT: 1.3×10^{-2} cm^{-1}) than those in DMNQ (8 mT) and MeONQ (8 mT). Relatively a small amount of population in the middle sublevel was obtained from the simulation. The middle sublevel was tentatively assigned to the in-plane T_z, since the ISC into the out-of-plane T_x would be the smallest in planar organic molecules. The ratio of the relative population differences was determined to be $(p_y - p_x):(p_z - p_x) = 0.9:0.1$ in the present quinone derivatives. Thus, the order of the triplet sublevels was assigned to be $T_y > 0 > T_z > T_x$ in energy.

In an MCH matrix, very strong emissive signals due to $|\Delta M_S| = 2$ transition and radical products ($g = 2.003$) were observed while the $|\Delta M_S| = 1$ transitions were relatively broad. Strong radical signals also were measured even at 4 K in an MCH matrix. These are probably due to hydrogen abstraction from the matrix molecules. The ZFS parameters listed in Table 1 and the component line width of the spectra in MCH are quite similar to those observed in an MTHF matrix.

In a toluene matrix, a relatively small $|D|$ value (0.176 cm^{-1}) and Gaussian line width (8 mT) were observed for MNQ compared with those in the other matrices. In contrast, the ZFS parameters of DMNQ and MeONQ were nearly identical to those in the MCH and MTHF matrices (Table 1).

TREPR measurements were also performed in alcoholic matrices to examine the effects of hydrogen bonding on the ZFS parameters. Figure 4 shows the TREPR spectra of the naphthoquinone derivatives in an absolute ethanol matrix. For MNQ, the $|\Delta M_S| = 2$ transition shifts to lower field and the line width becomes broader in comparison with the nonprotic matrices. The Gaussian line width of 20 mT was used to reproduce the spectrum of MNQ while they were 9 and 8 mT for DMNQ and MeONQ, respectively. Inhomogeneous distribution of the ZFS parameters may be responsible for the TREPR spectral features of MNQ. This is probably because the environment of the quinones is heterogeneous. On the other hand, for DMNQ and MeONQ, the hydrogen bond formation had little effect on the ZFS parameters. When undehydrated ethanol was used as a matrix, the TREPR spectra become significantly weaker but little effect on the ZFS parameters was observed.

4. Discussion

Since the phosphorescence spectrum of MNQ showed well-resolved vibrational structure even in alcohol matrices, the T_1 state is considered to be mainly $^3n\pi^*$ in character in protic matrices as well as in nonpolar matrices. The observed matrix dependence of the ZFS parameters clearly suggests the mixing of $^3\pi\pi^*$ character in the T_1 state through the spin-orbit interactions. The remarkable inhomogeneous broadening of the TREPR spectra observed indicates that the contribution of the spin−orbit interaction is heterogeneous in MNQ.

On the other hand, DMNQ and MeONQ showed broad phosphorescence spectra and the lifetimes were longer than those of NQ and MNQ. Little matrix effect on the ZFS parameters was observed in these quinones. These experimental facts lead to the conclusion that the T_1 states of DMNQ and MeONQ are mainly $^3\pi\pi^*$ in character. The assignment is also supported by the fact that the component line widths of the TREPR spectra of DMNQ and MeONQ are less than half of that in MNQ. Since $|D|$ values are relatively large in these quinones compared with those of the usual $^3\pi\pi^*$ states of hydrocarbons, it can be deduced that there exists weak spin-orbit coupling with the $^3n\pi^*$ state located at a higher energy. The change of the electron spin distribution gave negligible effect on the relative population difference in the triplet sublevel. This result indicates that the ISC process is dominantly governed by the spin-orbit interaction due to the carbonyl oxygen atoms. We conclude that the T_1 states of the present naphthoquinone derivatives have more or less mixed character of $^3n\pi^*$ and $^3\pi\pi^*$.

Semiempirical calculations using the INDO/1 algorithm were performed to confirm the substituent effects on the electronic structure of naphthoquinones.[27] The important upper occupied MOs and the lowest unoccupied MO of NQ obtained are shown in Figure 5. The HOMO is n_- MO in NQ. The LUMO and next LUMO are π_-^* and π'_-^*, respectively. Figure 6 depicts the dependence of the eigen values of the LUMO and the four highest occupied MOs on the substituted groups. Although the perturbation of a methyl group is negligible in MNQ, the π_+ MO is significantly close to the n_- MO in DMNQ. In MeONQ, the HOMO calculated is clearly the π_+ MO. The present results indicate that the electron donating groups at the 2 and 3 positions destabilize the π_+ orbital compared with the n_- MO, resulting in the stabilization of the $\pi_+\pi_-^*$ states more than the $n_-\pi_-^*$ states. Therefore, the main character of the T_1 states would be $^3\pi_+\pi_-^*$ state in DMNQ and MeONQ. It should be noted that the direct spin-orbit interaction between the $^3\pi_+\pi_-^*(B_2)$ and

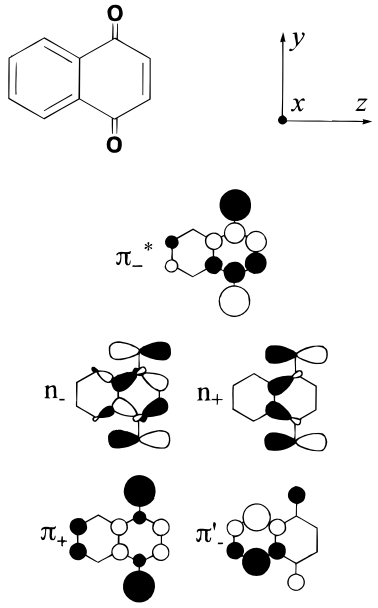

Figure 5. Pictorial representations of the LUMO and the four highest occupied MOs of NQ calculated by INDO method. Only the positions having the atomic coefficients more than 0.1 are described.

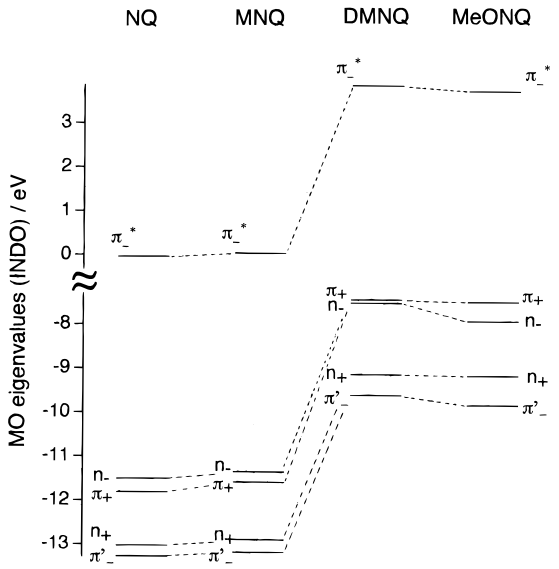

Figure 6. INDO correlation diagram for NQ, MNQ, DMNQ, and MeONQ.

$^3n_-\pi_-^*(B_1)$ states can be neglected because of the different symmetry. The important excited state coupled with the $^3n_-\pi_-^*$ state in MNQ would be the $^3\pi_-\pi_-^*(A_1)$ state located a little higher in energy.

The present results suggest that the T_1 states of the naphthoquinone derivatives have more or less mixed character of the $^3n\pi^*$ and $^3\pi\pi^*$ states. Thus, both electron spin dipolar interaction (D_{SS}) and spin-orbit interaction (D_{SO}) would contribute to the D value of the present systems. Based on the perturbation theory,[20] it has been pointed out that the D_{SO} value is proportional to the spin-orbit interaction matrix elements and inversely proportional to the energy gap (ΔE_T) between the $^3n\pi^*$ and $^3\pi\pi^*$ states. Formation of the hydrogen bond at the carbonyl oxygen atoms raises the energy level of $^3n\pi^*$ states. Since the T_1 state of MNQ is mainly $^3n\pi^*$ in character, the hydrogen-bonding interaction induces the reduction the ΔE_T, leading to the increase of the $|D|$ value. The wide distribution of the D value observed for MNQ in various matrices indicates that the D_{SO} value is very sensitive to the solute−matrix interaction for the quinones having mainly $^3n\pi^*$ character. The present work reveals that the triplet character 1,4-naphthoquinones is remarkably sensitive to the electron donating substituents in contrast to those of *p*-benzoquinones and 9,10-anthraquinones.

5. Summary

(1) The phosphorescence spectrum of MNQ showed well-resolved vibrational structures in various matrices, while in DMNQ and MeONQ broad spectra were observed even in a *n*-hexane matrix.

(2) The phosphorescence lifetimes were 0.14, 0.84, 1.4, and 4.2 ms for NQ[7], MNQ,[9] DMNQ,[7] and MeONQ in methanol/ethanol (1:1, v/v) at 77 K.

(3) The $|D|$ value of the ZFS parameters decreased with increasing the electron donating character of the substituent groups at the 2 and 3 positions of 1,4-naphthoquinone. In MNQ, the $|D|$ value depended on the matrix polarity, while in DMNQ and MeONQ minor matrix effect was observed. The component line widths of the TREPR spectra in MNQ were more than twice those in DMNQ and MeONQ.

(4) It has been concluded that the character of the T_1 state is mainly $^3n_-\pi_-^*$ in NQ and MNQ, while it is mainly $^3\pi_+\pi_-^*$ in DMNQ and MeONQ. However, the T_1 states of the present naphthoquinones are more or less mixed states of the $^3n\pi^*$ and $^3\pi\pi^*$ states by the spin-orbit coupling.

(5) The energy dependence of the MOs calculated by semiempirical method was consistent with the experimental results.

Acknowledgment. The present research was supported in part by Grants-in-Aid on Priority-Area-Research on Photoreaction Dynamics (No. 06239103) and of Scientific Research No. 07404040 from the Ministry of Education, Science, Sports and Culture, Japan.

References and Notes

(1) Patai, S.; Rappoport, Z. *The Chemistry of the Quinonoid Compounds*; John Wiley & Sons, New York, 1988.
(2) Itoh, T. *Chem. Rev.* **1995**, *95*, 2351, and references therein.
(3) Kuboyama, A. *Bull. Chem. Soc. Jpn.* **1978**, *51*, 2771.
(4) Kuboyama, A. *Bull. Chem. Soc. Jpn.* **1982**, *55*, 3635.
(5) Elliot, A. J.; Wan, J. K. S. *J. Phys. Chem.* **1978**, *82*, 444.
(6) Wong, S. K. *J. Am. Chem. Soc.* **1878**, *100*, 5488.
(7) Amada, I.; Yamaji, M.; Sase, M.; Shizuka, H. *J. Chem. Soc. Faraday Trans.* **1995**, *91*, 2751.
(8) Amada, I.; Yamaji, M.; Tsunoda, S.; Shizuka, H. *J. Photochem. Photobiol. A: Chem.* **1996**, *95*, 27.
(9) Amada, I.; Yamaji, M.; Sase, M.; Shizuka, H. *Res. Chem. Intermed.* **1997**, *23*, 121.
(10) Amada, I.; Yamaji, M.; Sase, M.; Shizuka, H.; Shimokage, T.; Tero-Kubota, S. *Res. Chem. Intermed.*, in press.
(11) Murai, H.; Minami, M.; Hayashi, T.; I'Haya, Y. J. *Chem. Phys.* **1985**, *93*, 333.
(12) Galaup, J. P.; Megel, J.; Trommsdorff, H. P. *J. Chem. Phys.* **1978**, *69*, 1030.
(13) Shimoishi, H.; Tero-Kubota, S.; Akiyama, K.; Ikegami, Y. *J. Phys. Chem.* **1989**, *93*, 5410.
(14) Lamola, A. A. *J. Chem. Phys.* **1967**, *47*, 4810.
(15) Case, W. A.; Kearns, D. R. *J. Chem. Phys.* **1970**, *52*, 2175.
(16) Li, Y. H.; Lim, E. C. *Chem. Phys. Lett.* **1971**, *7*, 15.
(17) Goodman, L.; Koyanagi, M. *Mol. Photochem.* **1972**, *4*, 369.
(18) Nishimura, A. M.; Tinti, D. S. *Chem. Phys. Lett.* **1972**, *13*, 278.
(19) Cheng, T. H.; Hirota, N. *Chem. Phys. Lett.* **1972**, *14*, 415.
(20) Hayashi, H.; Nagakura, S. *Mol. Phys.* **1972**, *24*, 801.
(21) Jones, C.; Maki, A. H.; Kearns, D. R. *J. Chem. Phys.* **1973**, *59*, 873.
(22) Cheng, T. H.; Hirota, N. *Mol. Phys.* **1974**, *27*, 281.
(23) Nakayama, T.; Sakurai, K.; Ushida, K.; Hamanoue, K.; Otani, A. *J. Chem. Soc., Faraday Trans.* **1991**, *87*, 449.
(24) Nakayama, T.; Sakurai, K.; Hamanoue, K.; Otani, A. *J. Chem. Soc., Faraday Trans.* **1991**, *87*, 1509.
(25) Fieser, L. F. *J. Am. Chem. Soc.* **1926**, *48*, 2922.
(26) Tero-Kubota, S.; Akiyama, K.; Ikoma, T.; Ikegami, Y. *J. Phys. Chem.* **1991**, *95*, 766.
(27) The semiempirical calculations were carried out by ZINDO of CAChe system.